Materials Letters 181 (2016) 38–41

Contents lists available at ScienceDirect

Materials Letters

journal homepage: www.elsevier.com/locate/matlet

Preparation of $NaSrLa(WO_4)_3$:Ho^{3+}/Yb^{3+} ternary tungstates and their upconversion photoluminescence properties

Chang Sung Lim [a,*], Victor V. Atuchin [b,c,d], Aleksandr S. Aleksandrovsky [e], Maxim S. Molokeev [f,g]

[a] Department of Advanced Materials Science & Engineering, Hanseo University, Seosan 356-706, Republic of Korea
[b] Laboratory of Optical Materials and Structures, Institute of Semiconductor Physics, SB RAS, Novosibirsk 630090, Russia
[c] Functional Electronics Laboratory, Tomsk State University, Tomsk 634050, Russia
[d] Laboratory of Semiconductor and Dielectric Materials, Novosibirsk State University, Novosibirsk 630090, Russia
[e] Laboratory of Coherent Optics, Kirensky Institute of Physics, SB RAS, Krasnoyarsk 660036, Russia
[f] Laboratory of Crystal Physics, Kirensky Institute of Physics, SB RAS, Krasnoyarsk 660036, Russia
[g] Department of Physics, Far Eastern State Transport University, Khabarovsk 680021, Russia

ARTICLE INFO

Article history:
Received 20 March 2016
Received in revised form
18 May 2016
Accepted 26 May 2016
Available online 2 June 2016

Keywords:
Tungstate
Phosphor
Sol-gel preparation
Luminescence
Raman spectroscopy
XRD

ABSTRACT

$NaSrLa_{1-x}(WO_4)_3$:Ho^{3+}/Yb^{3+} ternary tungstates were synthesized via microwave sol-gel route. Well-crystallized particles with particle sizes of 2–5 μm were obtained after heat-treatment at 900 °C for 16 h. Under the excitation at 980 nm, the particles showed yellow emissions based on the strong 545 and 655 nm emission bands. The preferable Yb^{3+}:Ho^{3+} ratio was obtained to be 9:1. Raman spectra of the doped particles indicated the presence of strong Ho^{3+} luminescence lines. The pump power dependence and Commission Internationale de L'Eclairage chromaticity of the upconversion emission intensity were evaluated.

1. Introduction

Inorganic luminescent materials are of great importance for modern photonic technologies and different phosphors with specific spectroscopic parameters were found in the recent years [1–9]. Binary alkaline earth tungstates $MLn_2(WO_4)_4$ (M: alkaline earth bivalent metal ion, Ln: trivalent rare-earth ions) belong to a group of scheelite-structured compounds. The scheelite-structured binary molybdates and tungstates have been reported in terms of excellent UC photoluminescence properties [9,10]. In particular, the rare-earth-doped binary $NaLn(WO_4)_2$ compounds possess the tetragonal phase with the space group $I4_1/a$ and belong to the family of scheelite-type structure. It is well employed for the trivalent rare-earth ions in the disordered tetragonal-phase to be partially substituted by Ho^{3+} and Yb^{3+} ions in the lanthanide site of Ln^{3+} [11–13].

Among the rare-earth ions, the Ho^{3+} ion is a suitable activator due to its intense green emission of $^5S_2/^5F_4 \rightarrow {}^5I_8$ transition and strong red emission of $^5F_5 \rightarrow {}^5I_8$ transition upon 980 nm excitation, while the sensitizer Yb^{3+} enhances the UC luminescence efficiency owing to its strong absorption around 980 nm. The co-doped Yb^{3+} ion and Ho^{3+} ion can remarkably enhance the UC efficiency due to the efficient energy transfer from Yb^{3+} to Ho^{3+} [11–13]. The ternary tungstates with general composition $NaMLn(WO_4)_3$ (M = Ca^{2+}, Sr^{2+} and Ba^{2+}, and Ln = La^{3+}, Gd^{3+} and Y^{3+}) have not been reported up to now. As compared to the common technological methods, microwave synthesis has its advantages of a very short reaction time, small-size particles, narrow particle size distribution, and high purity of final polycrystalline samples purity [14,15]. In the present study, the ternary tungstate $NaSrLa_{1-x}(WO_4)_3$:Ho^{3+}/Yb^{3+} phosphors with the proper doping concentrations of Ho^{3+} and Yb^{3+} (x = Ho^{3+} + Yb^{3+}, Ho^{3+} = 0, 0.05, 0.1, 0.2, and Yb^{3+} = 0, 0.2, 0.45) were successfully prepared by the microwave sol-gel method followed by heat treatment in the air. The particles were characterized by X-ray diffraction (XRD) and scanning electron microscopy (SEM). The optical properties were examined using photoluminescence (PL) emission and Raman spectroscopy. The synthesis and measurement conditions can be found in Supporting Information.

* Corresponding author.
E-mail address: cslim@hanseo.ac.kr (C.S. Lim).

http://dx.doi.org/10.1016/j.matlet.2016.05.121
0167-577X/

2. Results and discussion

The XRD patterns of the samples are shown in Fig. 1. In the synthesized samples, almost all XRD peaks were indexed by tetragonal phase with parameters close to $SrWO_4$ (JCPDS 08-0490). Therefore, the synthesized $NaSrLa(WO_4)_3$ particles belong to tungstate family with a scheelite-type structure. The crystal structure of $SrWO_4$ was taken as the starting model for Rietveld refinement using package TOPAS 4.2. As shown in Fig. 1S, the defined crystal structure contains WO_4 tetrahedrons coordinated by four $(Sr/Na/La/Ho/Yb)O_8$ square antiprisms. The refinements were stable and give low R-factors (Tables 1S–3S, Figs. 2S–5S). The linear cell volume increasing per average ion radii IR(Na/Sr/La/Ho/Yb) proves the suggested chemical formulas (Fig. 6S) [16]. Consequently, the Ho^{3+} and Yb^{3+} ions can be efficiently incorporated into the $NaSrLa(WO_4)_3$ lattice by partial substitution for La^{3+}. Thus, the post heat-treatment at 900 °C for 16 h plays an important role in reaching of the precursor crystallization.

The SEM images of the $NaSrLa_{0.8}(WO_4)_3$:$Ho_{0.2}$ and $NaSrLa_{0.50}(WO_4)_3$:$Ho_{0.05}Yb_{0.45}$ particles are provided in Fig. 2. The as-synthesized samples possess the homogeneous morphology and particle size of 2–5 μm. The partly agglomerated particles are induced by the atom inter-diffusions between the grains. The morphology feature is insensitive to the Ho^{3+}/Yb^{3+} doping concentrations. This suggests that the microwave sol-gel route is suitable for the creation of homogeneous $NaSrLa_{1-x}(WO_4)_3$:xHo^{3+}/Yb^{3+} crystallites.

Fig. 3 shows the UC photoluminescence emission spectra of the samples excited under 980 nm. The $NaSrLa_{0.7}(WO_4)_3$:$Ho_{0.1}Yb_{0.2}$ and $NaSrLa_{0.50}(WO_4)_3$:$Ho_{0.05}Yb_{0.45}$ particles exhibited yellow emissions based on the strong 545 and 655 nm emission bands. The UC intensities of $NaSrLa(WO_4)_3$ and $NaSrLa_{0.8}(WO_4)_3$:$Ho_{0.2}$ particles were not detected. The UC intensity of $NaSrLa_{0.50}(WO_4)_3$:$Ho_{0.05}Yb_{0.45}$ is much higher than that of $NaSrLa_{0.7}(WO_4)_3$:$Ho_{0.1}Yb_{0.2}$. The strong 545-nm emission band in the green region corresponds to the $^5S_2/^5F_4 \rightarrow {}^5I_8$ transition, while the very strong emission 655-nm band in the red region corresponds to the $^5F_5 \rightarrow {}^5I_8$ transition [17,18]. The Ho^{3+} ion activator is the luminescence center for these UC samples, and the sensitizer Yb^{3+} enhances the UC luminescence intensity because of the efficient energy transfer from Yb^{3+} to Ho^{3+}. The schematic energy level diagrams of $Yb^{3+}$and Ho^{3+} ions is shown in Fig. 7S. With increase of the Ho^{3+} and Yb^{3+} concentrations, the distance between Ho^{3+} and Yb^{3+} ions decreases, which can promote non-radiative energy transfer [19,20]. As shown in Fig. 3, the higher intensity of $NaSrLa_{0.50}(WO_4)_3$:$Ho_{0.05}Yb_{0.45}$ is found at Yb^{3+}:Ho^{3+} = 9:1, and, thus, the preferable Yb^{3+}:Ho^{3+} ratio is as high as 9:1.

The insert in Fig. 3 shows logarithmic scale dependence of the UC emission intensities at 545 and 655 nm on the working pump power over the range of 20–110 mW in the $NaSrLa_{0.50}(WO_4)_3$:$Ho_{0.05}Yb_{0.45}$ sample. The UC emission intensity I is proportional to the slope value n of the irradiation pumping power P, where n is the number of pumped photons required to produce UC emission [20]:

$$I \propto P^n \tag{1}$$

$$\mathrm{Ln}\ I \propto n\ \mathrm{Ln}\ P \tag{2}$$

As evident from Fig. 4, the slope values are $n = 1.74$ for green emission at 545 and $n = 1.84$ for red emission at 655 nm, respectively. These results show that the UC mechanism can be explained by a two-photon UC process in Ho^{+3}/Yb^{3+} co-doped phosphors.

The calculated chromaticity coordinates and CIE chromaticity diagram are shown in Fig. 8S. The inset shows the chromaticity points for the samples. The chromaticity coordinates (x, y) are strongly dependent on the Ho^{3+}/Yb^{3+} concentration ratio. As shown in Fig. 4, the calculated chromaticity coordinates for $NaSrLa_{0.7}(WO_4)_3$:$Ho_{0.1}Yb_{0.2}$ and $NaSrLa_{0.50}(WO_4)_3$:$Ho_{0.05}Yb_{0.45}$ correspond to the yellow region in CIE diagram.

The Raman spectra of the synthesized samples are shown in Fig. 4. The sharp internal modes for the pure $NaSrLa(WO_4)_3$ were detected at 192, 328, 378,830 and 920 cm^{-1} that indicates high crystallinity of the particles. The Raman spectrum of the $NaSrLa(WO_4)_3$ shows the typical tungstate configuration with a wide empty gap over 400–800 cm^{-1} [21,22]. The band at 920 cm^{-1} corresponds to stretching vibrations of the

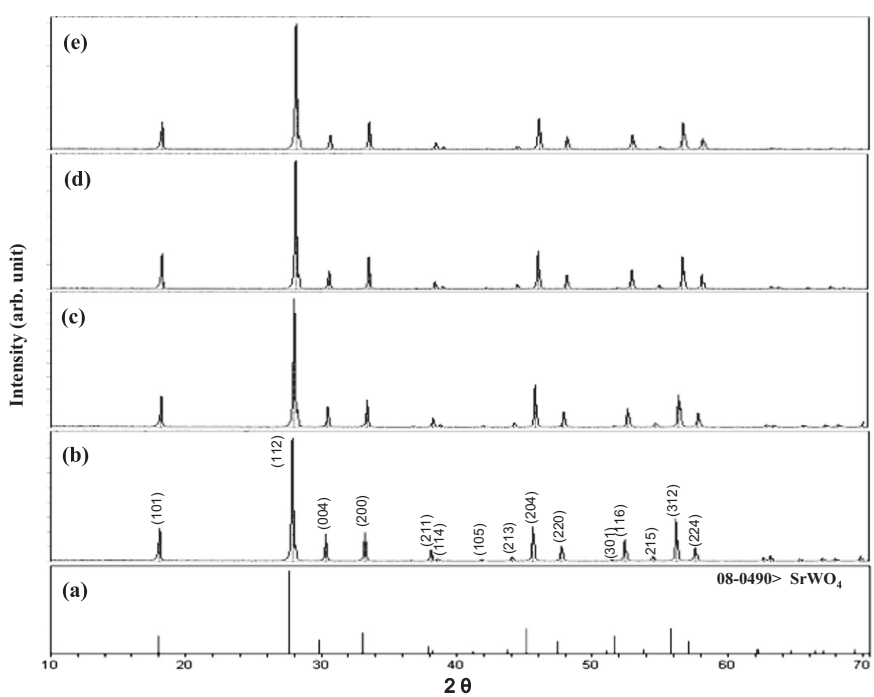

Fig. 1. XRD patterns of the (a) JCPDS 08-0490 pattern of $SrWO_4$, (b) pure $NaSrLa(WO_4)_3$, (c) $NaSrLa_{0.8}(WO_4)_3$:$Ho_{0.2}$, (d) $NaSrLa_{0.7}(WO_4)_3$:$Ho_{0.1}Yb_{0.2}$, and (e) $NaSrLa_{0.50}(WO_4)_3$:$Ho_{0.05}Yb_{0.45}$ particles.

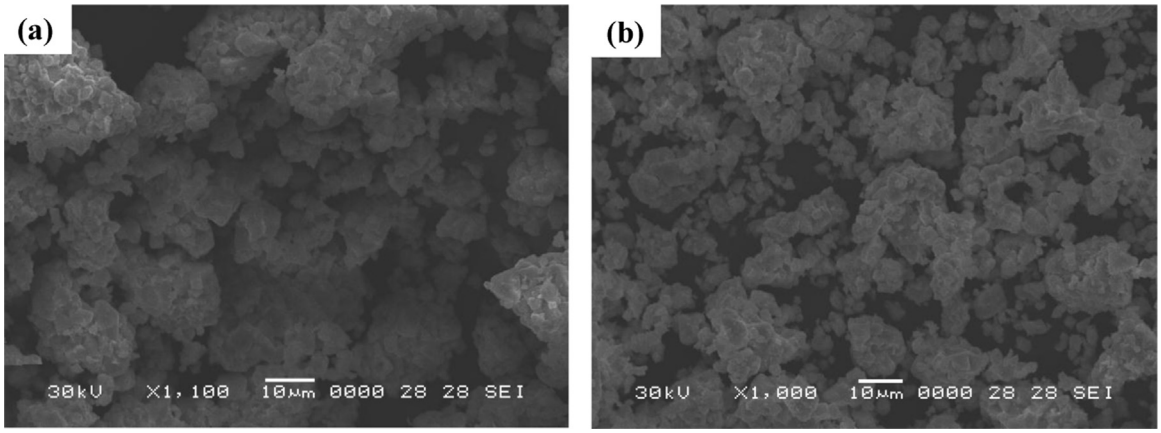

Fig. 2. SEM images of the (a) $NaSrLa_{0.8}(WO_4)_3$:$Ho_{0.2}$ and (b) $NaSrLa_{0.50}(WO_4)_3$:$Ho_{0.05}Yb_{0.45}$ particles.

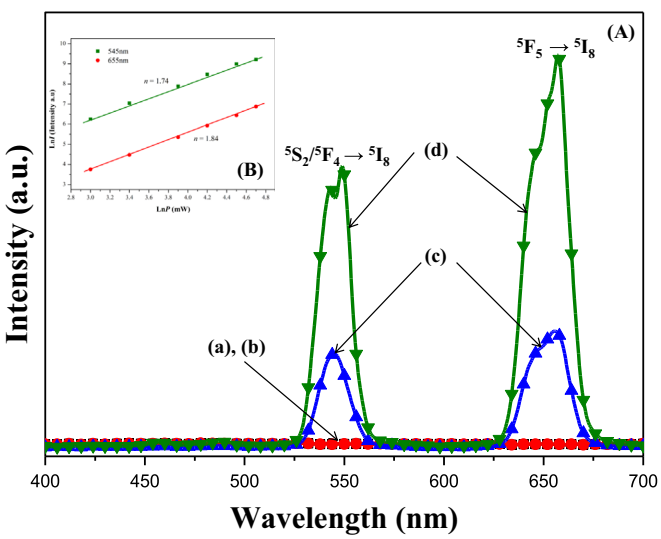

Fig. 3. (A) UC photoluminescence emission spectra of (a) $NaSrLa(WO_4)_3$, (b) $NaSrLa_{0.8}(WO_4)_3$:$Ho_{0.2}$, (c) $NaSrLa_{0.7}(WO_4)_3$:$Ho_{0.1}Yb_{0.2}$ and (d) $NaSrLa_{0.50}(WO_4)_3$:$Ho_{0.05}Yb_{0.45}$ particles excited under 980 nm. The insert (B) shows logarithmic scale dependence of the UC emission intensity on the pump power in the range of 20–110 mW in $NaSrLa_{0.50}(WO_4)_3$:$Ho_{0.05}Yb_{0.45}$ sample.

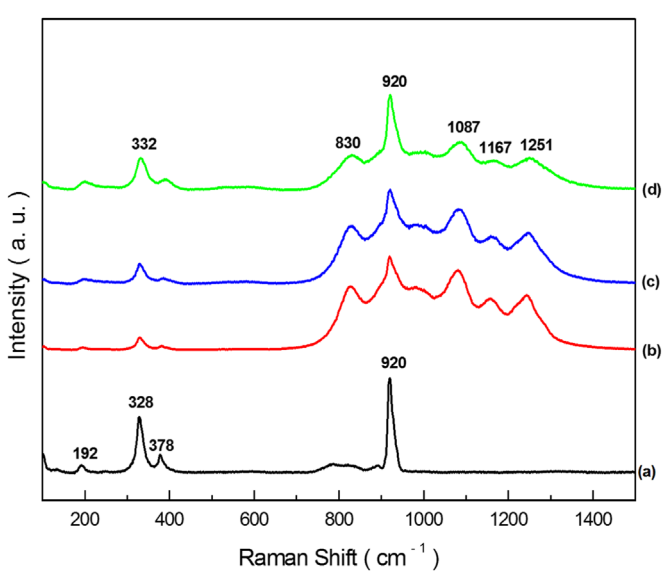

Fig. 4. Raman spectra of (a) pure $NaSrLa(WO_4)_3$, (b) $NaSrLa_{0.8}(WO_4)_3$:$Ho_{0.2}$, (c) $NaSrLa_{0.7}(WO_4)_3$:$Ho_{0.1}Yb_{0.2}$, and (d) $NaSrLa_{0.50}(WO_4)_3$:$Ho_{0.05}Yb_{0.45}$.

WO_4 tetrahedra. The band at 328 and 378 cm^{-1} could be assigned to the longer W–O bonds vibrations. The La^{3+} translations are located at below 180 cm^{-1} [23–25]. The Raman spectra of the doped particles indicate the dominant peaks at wavenumbers above 830 cm^{-1}. According to Raman spectra of the doped samples recorded under the excitation at 514.5-nm, the Raman lines are superimposed by strong Ho^{3+} luminescence lines.

3. Conclusion

The $NaSrLa(WO_4)_3$:Ho^{3+}/Yb^{3+} ternary tungstate phosphors were successfully synthesized via microwave sol-gel route. With excitation at 980 nm, the $NaSrLa_{0.7}(WO_4)_3$:$Ho_{0.1}Yb_{0.2}$ and $NaSrLa_{0.50}(WO_4)_3$:$Ho_{0.05}Yb_{0.45}$ particles showed yellow emissions based on a combination of 545 and 655 nm emission bands, which were assigned to the $^5S_2/^5F_4 \rightarrow {}^5I_8$ and $^5F_5 \rightarrow {}^5I_8$ transitions, respectively. The preferable Yb^{3+}:Ho^{3+} ratio is 9:1. The Raman spectra of the doped particles indicated the domination of strong peaks at higher frequencies induced by the strong Ho^{3+} luminescence lines. These results led to high emitting efficiency and the involved materials can be considered as potentially active components in new optoelectronic devices and in the field of luminescent imaging.

Acknowledgments

This research was supported by the Basic Science Research Program through the National Research Foundation of Korea (NRF) funded by the Ministry of Education (2015-058813), SB RAS Program No.II.2P (No. 0358-2015-0012) and Russian Foundation for Basic Research (15-52-53080).

Appendix A. Supplementary material

Supplementary data associated with this article can be found in the online version at http://dx.doi.org/10.1016/j.matlet.2016.05.121.

References

[1] G.G. Li, Y. Tian, Y. Zhao, J. Lin, Chem. Soc. Rev. 44 (2015) 8688–8713.
[2] Z.G. Xia, R.-S. Liu, K.-W. Huang, V. Drozd, J. Mater. Chem. 22 (2012) 15183–15189.
[3] J. Beltran-Huarac, J.Z. Wang, H. Tanaka, W.M. Jadwisienczak, B.R. Weiner,

G. Morell, J. Appl. Phys. 114 (2013) 053106.
[4] Z.G. Xia, Y.Y. Zhang, M.S. Molokeev, V.V. Atuchin, J. Phys. Chem. C 117 (2013) 20847–20854.
[5] A.V. Malakhovskii, T.V. Kutsak, A.L. Sukhachev, A.S. Aleksandrovsky, A. S. Krylov, I.A. Gudim, M.S. Molokeev, Chem. Phys. 428 (2014) 137–143.
[6] Y.X. Zhuang, Y. Katayama, J. Ueda, S. Tanabe, Opt. Mater. 36 (2014) 1907–1912.
[7] V.V. Atuchin, N.F. Beisel, E.N. Galashov, E.M. Mandrik, M.S. Molokeev, A. P. Yelisseyev, A.A. Yusuf, Z.G. Xia, ACS Appl. Mater. Interfaces 7 (2015) 26235–26243.
[8] S.Q. Liu, Y.J. Liang, Y.L. Zhu, X.G. Wu, R. Xu, M.H. Tong, Opt. Laser Technol. 84 (2016) 1–8.
[9] C.S. Lim, A. Aleksandrovsky, M. Molokeev, A. Oreshonkov, V. Atuchin, Phys. Chem. Chem. Phys. 17 (2015) 19278–19287.
[10] C.S. Lim, Mater. Res. Bull. 75 (2016) 211–216.
[11] L. Li, W. Zi, H. Yu, S. Gan, G. Ji, H. Zou, X. Xu, J. Lumin. 143 (2013) 14–20.
[12] C. Ming, F. Song, L. Yan, Opt. Commun. 286 (2013) 217–220.
[13] N. Xue, X. Fan, Z. Wang, M. Wang, J. Phys. Chem. Solids 69 (2008) 1891–1896.
[14] C.S. Lim, Ceram. Int. 41 (2015) 12464–12470.
[15] C.S. Lim, V. Atuchin, A. Aleksandrovsky, M. Molokeev, A. Oreshonkov, J. Am. Ceram. Soc. 98 (2015) 3223–3230.
[16] R.D. Shannon, Acta Cryst. A 32 (1976) 751–767.
[17] D.A. Ikonnikov, A.V. Malakhovskii, A.L. Sukhachev, V.L. Temerov, A.S. Krylov, A. F. Bovina, A.S. Aleksandrovsky, Opt. Mater. 37 (2014) 257–261.
[18] F. Anzel, G. Baldacchini, L. Laversenne, G. Boulon, Opt. Mater. 24 (2003) 103–109.
[19] W. Lu, L. Cheng, J. Sun, H. Zhong, X. Li, Y. Tian, J. Wan, Y. Zheng, L. Huang, T. Yu, H. Yu, B. Chen, Physica B 405 (2010) 3284–3288.
[20] H. Guo, N. Dong, M. Yin, W. Zhang, L. Lou, S. Xia, J. Phys. Chem. B 108 (2004) 19205–19209.
[21] T.T. Basiev, A.A. Sobel, Y.K. Voronko, P.G. Zverev, Opt. Mater. 15 (2000) 205–216.
[22] V.V. Atuchin, V.G. Grossman, S.V. Adichtchev, N.V. Surovtsev, T.A. Gavrilova, B. G. Bazarov, Opt. Mater. 34 (2012) 812–816.
[23] V.V. Atuchin, O.D. Chimitova, T.A. Gavrilova, M.S. Molokeev, Sung-Jin. Kim, N. V. Surovtsev, B.G. Bazarov, J. Cryst. Growth 318 (2011) 683–686.
[24] V.V. Atuchin, O.D. Chimitova, S.V. Adichtchev, J.G. Bazarov, T.A. Gavrilova, M. S. Molokeev, N.V. Surovtsev, Zh.G. Bazarova, Mater. Lett. 106 (2013) 26–29.
[25] C.S. Lim, A. Aleksandrovsky, M. Molokeev, A. Oreshonkov, V. Atuchin, J. Solid State Chem. 228 (2015) 160–166.